Reconciling Differences in Post-Flight Trajectory Reconstruction for EDL Applications

Jason A. Corman*

Georgia Institute of Technology, Atlanta, Georgia, 30332, United States

Post-flight trajectory reconstruction for planetary entry, descent, and landing (EDL) missions has played an essential role in the improvement of planetary exploration, because it allows researchers to assess vehicle system performance and atmospheric conditions during flight. Mars Science Laboratory (MSL) will be the first Mars entry vehicle to contain pressure sensing equipment embedded in the heatshield to support trajectory reconstruction, which brings new opportunities and challenges in the area. There have been a number of reconstruction methods developed during past missions, and these methods are being examined in preparation for MSL to determine the level of accuracy in which particular variables of vehicle performance can be estimated. To assess this accuracy and provide further insights into the capability of reconstruction, it is desirable to reconcile differences between the respective trajectories estimated by each method. This paper discusses the challenges associated with trajectory reconciliation and various statistical and deterministic techniques in which it can be performed. Recommendations are made that discuss the most viable options for reconciliation and a baseline process by which to incorporate those options is presented and demonstrated using 3-DOF trajectory simulation and reconstruction models.

*Graduate Research Assistant, NASA LaRC Graduate Student Research Program

Executive Summary

In post-flight reconstruction of entry, descent, and landing missions, there are multiple methods that make different use of available measurement data. Each of these methods generate an estimate of vehicle state variables over the entire time-series of the trajectory, and the accuracy of these estimations is significantly important to validate and further develop pre-flight simulation capabilities. If each reconstructed trajectory is unique, however, reconciliation of differences between state variable estimations can provide meaningful information to support that accuracy assessment. This proves to be a difficult task because requirements are enforced along the entire time span of the trajectory and therefore the problem is driven to comparing multivariate time-series data.

Various techniques to perform trajectory reconciliation are discussed in this paper (Section IV), but there is one combination of methods that presents the greatest potential to produce insightful results. Functional data enabled Bayesian calibration is an approach that is anticipated to reconcile simulation and testing data without the need for significant data reduction. Bayesian calibration for this application would focus on determining the distribution of calibration variables in order to interpret their physical meaning with a level of confidence and help understand shortcomings of specific reconstruction techniques. However, this Bayesian approach depends on regression or surrogate modeling of the data, and it becomes immediately apparent that a solution to this problem ultimately relies on the ability to parametrically regress time-dependent multivariate data. This is an entire area of research in itself and outside the scope of this paper, but there is anticipated to be a more tangible short-range solution. Semi-parametric functional models allow for time-dependent regression of a single response and therefore can support Bayesian calibration for the entire time-series for one of the reconstructed state variables.

The other option presented by functional data analysis is the ability to visually represent the data in an easily interpretable manner. The process described in Section V is a recommended baseline to perform reconciliation that begins with exploratory analysis of the data that incorporates visually quantitative and qualitative techniques. This important step in the reconciliation process can provide a better understanding of correlation of variables, uncertainty propagation, and intricate functional form of the data and gives subject matter experts a means to support their engineering judgment. It can also enable graphical reconciliation methods such as profile and pattern matching. A procedure for validation is also presented in this process, and other general comments on feasibility, advantages, disadvantages, etc. regarding the reconciliation of multivariate time-dependent data can be found throughout the paper.

Nomenclature

$\mathbf{X}$ = Generic Vehicle State Vector
$\mathbf{X}'_i$ = Reconstructed Trajectory of i-th Reconstruction Method
L/D = Lift-to-Drag Ratio
$\mathbf{w}$ = Input Vector of Uncertain Variables
α = Vehicle Orientation, angle of attack (deg)
β = Vehicle Orientation, sideslip angle (deg)
σ = Vehicle Orientation, roll angle (deg)
r = Vehicle Position, radial altitude (m)
ϕ_r = Vehicle Position, latitude (deg)
θ_r = Vehicle Position, longitude (deg)
V_{xI} = Vehicle Inertial X-Velocity (m/s)
V_{yI} = Vehicle Inertial Y-Velocity (m/s)
V_{zI} = Vehicle Inertial Z-Velocity (m/s)
ω_x = Vehicle Angular Rate, X (deg/s)
ω_y = Vehicle Angular Rate, Y (deg/s)
ω_z = Vehicle Angular Rate, Z (deg/s)
M_∞ = Freestream Mach Number
q_∞ = Freestream Dynamic Pressure, Pa
p = Size of Input Vector, $\mathbf{w}$

I. Introduction

The importance of post-flight trajectory reconstruction for Mars entry, descent, and landing (EDL) missions has been well established since its inception during the Viking era. By processing measurements collected during EDL, vehicle flight parameters and atmospheric conditions can be estimated to help validate and improve pre-flight simulation capabilities. For the Mars Science Laboratory mission, several different reconstruction techniques have been developed from previous missions and various research, and each technique will generate a possibly unique reconstructed trajectory, $\mathbf{X}'_i(t)$. Determining causality of differences between these trajectories can provide insight into the accuracy of current reconstruction techniques as well as capabilities of pre-flight simulations.

Since the design and testing of Mars vehicles and development of new technologies rely very heavily upon computational simulations, validation of these capabilities is of utmost importance. As Braun and Manning mention in their 2007 paper, for successful human exploration of the Mars surface, the landing footprint of the entry vehicle must be reduced to the order of 10's of meters and be expanded to carry a surface payload of 40-80 metric tons.[1] This type of mission improvement requires significant development of newer technologies, and cycle time of technology performance validation and certification is decreased as greater confidence is instilled in simulation models. Therefore, motivation for trajectory reconciliation is apparent, but the difficulties in performing the actual process are not necessarily so transparent.

This paper will introduce the complications and challenges involved with reconciling differences between EDL trajectories by briefly reviewing current resources available in modeling and simulation for the prediction and reconstruction of trajectories. The impact of uncertainty within the entire reconciliation process will also be addressed, and deterministic and statistical method of reconciliation will be introduced, highlighting the advantages and disadvantages of each. Based on this assessment, recommendations will be made as to which method is most applicable and/or feasible. Finally, a baseline process of reconciliation will be demonstrated on 3-DOF trajectory prediction and reconstruction models.

II. Trajectory Simulation

In the context of entry, descent, and landing, a trajectory is a collection of variables that explain the state of the vehicle, i.e. a state vector $\mathbf{X}$, over time. This paper will refer to trajectories in the same manner as Christian and Bruan, where three distinct trajectories are described:

Nominal Pre-flight expectation of the state vector over time during EDL using nominal conditions,

True Actual state of vehicle during flight, which can be measured but is essentially unknown, and

Reconstructed Post-flight estimation of vehicle state based on measurements taken during the true trajectory.

The state can be described by a number of both local and global variables, and a representative state vector used in pre-flight simulation can be formulated as

$$\mathbf{X} \equiv (r, \phi_r, \theta_r, \alpha, \beta, \sigma, V_{xI}, V_{yI}, V_{zI}, \omega_x, \omega_y, \omega_z)^T. \tag{1}$$

The nominal trajectory is predicted by a forward numerical integration of the equations of motion that updates the variables in this state vector at each time step, and there are a number of models and algorithms that must be incorporated into the simulation in order for successful and accurate integration.

The Program to Optimize Simulated Trajectories (POST) is the standard for pre-flight trajectory simulation and possesses the capability for three-degree-of-freedom or six-degree-of-freedom analyses.[2] POST utilizes surrogates for vehicle performance in lieu of higher-fidelity and computationally expensive analyses such as CFD or FEA. One of the most leveraged resources is the aerodynamic database, which tabulates aerodynamic coefficients, i.e. C_N, C_A, and C_m, for various Mach numbers, angles of attack, and sideslip angles. This database is typically integrated into the simulation as a linear interpolation model, and a graphical representation of those models for a vehicle similar to MSL are shown in Fig 1. Development of the aerodynamic database most heavily relies on computational fluid dynamics but is also validated with wind tunnel and ballistic range testing as well as applicable "heritage" information, i.e. past trajectory reconstructions of vehicles within the same technology and flight envelopes. Because these validation techniques are limited by Mach numbers, gas chemistries, vehicle orientations, and budget/facilities constraints, there is an inherent uncertainty within the aerodynamic database that needs to be accounted for during simulation, reconstruction, and the reconciliation of trajectories. For more information, refer to studies of wind tunnel testing used for validation and uncertainty quantification for Viking[3] and Phoenix.[4]

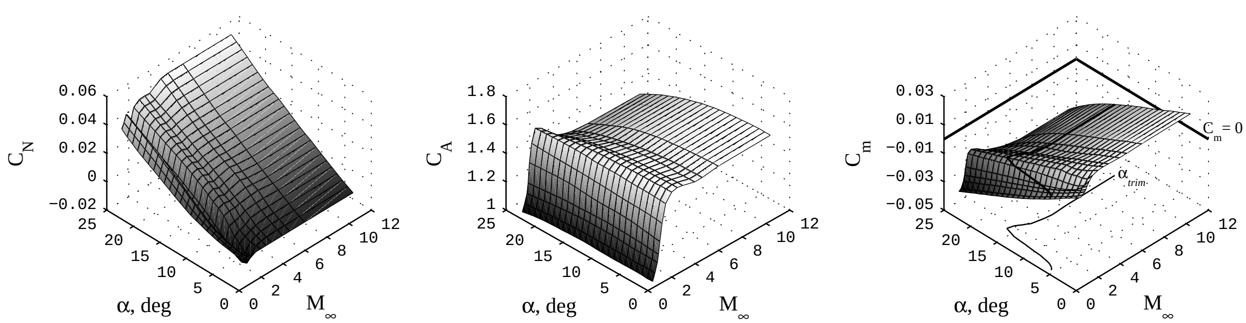

(a) Normal (b) Axial (c) Pitching Moment

Figure 1. Shown in this figure are interpolation models of an aerodynamic database for values of α between 0 and 23 degrees and Mach numbers from 0.4 to 10.35 of a vehicle similar to Mars Science Laboratory. Increased L/D is witnessed with increases in α when examining the relationship of (a) and (b), and the trim angle of attack, α_{trim}, for this particular vehicle is shown where the pitching moment coefficient, $C_m = 0$ (c).

Pre-flight simulation with POST also contains planetary information with stochastic atmospheric models, the ability for variation and transformation of coordinate systems, optimization algorithms, guidance/navigation/control, propulsion systems, and parachute simulations. Although vast improvements have been made in trajectory predictive capabilities, uncertainty exists in lower level inputs such as:

– vehicle mass properties (c.g. offsets, moments of inertia),

– state of vehicle at atmospheric entry (velocity, flight-path angle, altitude),
– timing of control maneuvers (ballast ejection, parachute deploy, heatshield separation),
– hardware bias (radar altimeter, inertial measuring unit),

as well as modeling considerations:

– atmospheric conditions (pressure, temperature, and density profiles),
– aerodynamic database (normal, axial, and pitching moment coefficients), and
– simplifying assumptions (3-DOF simulation, lower order linear models and interpolations).

These uncertainties are important in the reconciliation process because ultimately, differences in trajectories will be attributed to them. A more specific and comprehensive list of uncertainties with 3-σ bounds can be found in Striepe et al.[5] and Desai et al.,[6] and sensitivity studies are seen in the "Results and Discussion" section of Braun et al.[7] Further information can be found for general pre-flight simulation and results for Viking,[8] MPF,[7] MER,[6,9,10] and Phoenix.[11–13]

III. Trajectory Reconstruction

A significant amount of planning is underway to prepare for trajectory reconstruction of Mars Science Laboratory EDL. Since the vehicle heatshield is fitted with the Mars Entry Atmospheric Data System (MEADS), reconstruction analysts will be able to utilize forebody pressure measurements for the first time in Mars flight. Because of the heritage of the Shuttle Entry Air Data System (SEADS), it is anticipated that the pressure data will support more accurate reconstruction of aerodynamic state variables,

$$\mathbf{X}' = (\alpha, \beta, M_\infty, q_\infty)^T \tag{2}$$

and offer an independent method from traditional reconstruction techniques. Along with pressures, data from the inertial measuring unit (accelerations, rates, quaternions), radar altimetry and surface imaging will also be available, and the anticipated flow of information for MSL reconstruction efforts is shown in Fig. 2. The following subsections describe the estimation process for the state variables in Eqn. 2.

A. Aerodynamic Database

The use of aerodynamic databases for trajectory prediction and reconstruction in EDL is dated back to the first space shuttle and Viking missions. Reconstruction using the aerodynamic database is enabled by acceleration measurements taken by the IMU. Gnoffo[14] et al.

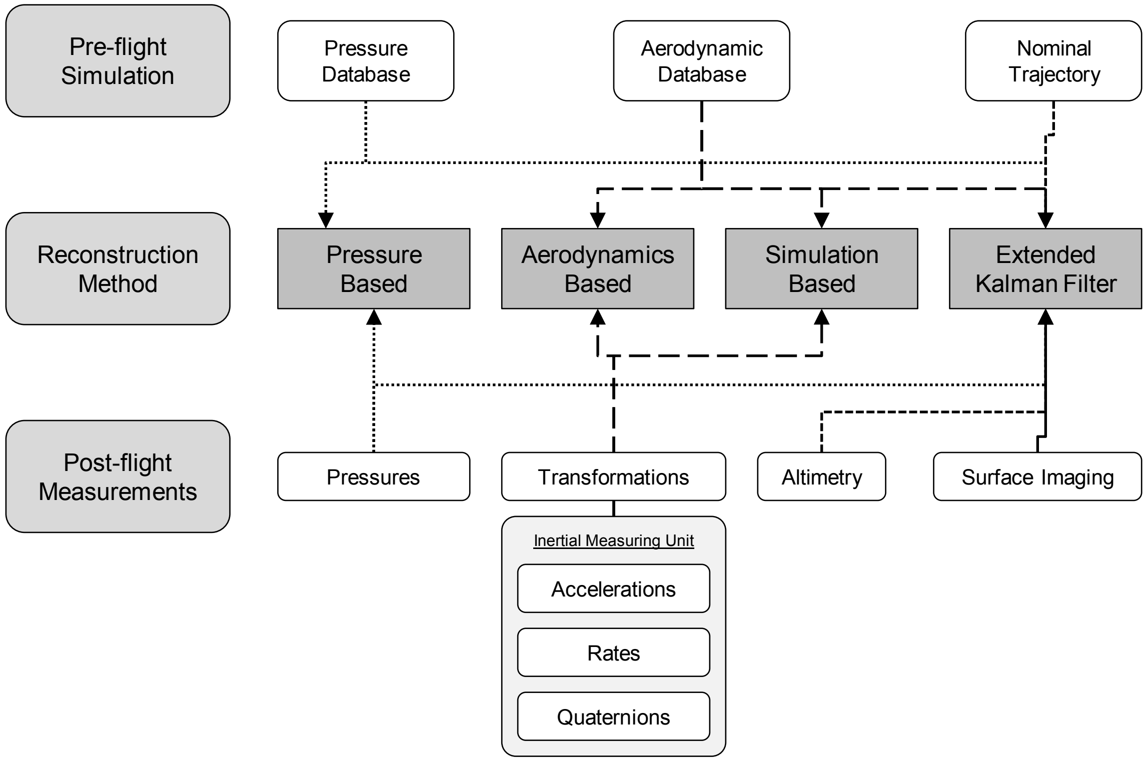

Figure 2. The flow of information for trajectory reconstruction shows which sources of pre-flight simulations and post-flight measurements are used by each method.

has shown that the direct relationship between accelerations and aerodynamic coefficients, as seen in Eqn. 3, can be used to estimate the entire time-series of total angle of attack.

$$\frac{A_N}{A_A} = \left(\frac{m_v A_N}{0.5\rho\infty V_\infty^2 S}\right)\left(\frac{0.5\rho\infty V_\infty^2 S}{m_v A_A}\right)\frac{C_N}{C_A} \tag{3}$$

where

$$A_N = \sqrt{A_X + A_Y} \tag{4}$$

with A_X and A_Y representing the acceleration in the vertical and horizontal vehicle coordinate axes, and a 3-DOF representation of vehicle and free-stream coordinates can be seen in Figure 3.

Estimation of other aerodynamic state variables requires the use of atmospheric models for pressure and density. Free-stream density can be estimated by

$$\rho_\infty = \frac{2m_A A_A}{V_\infty^2 C_A S} \tag{5}$$

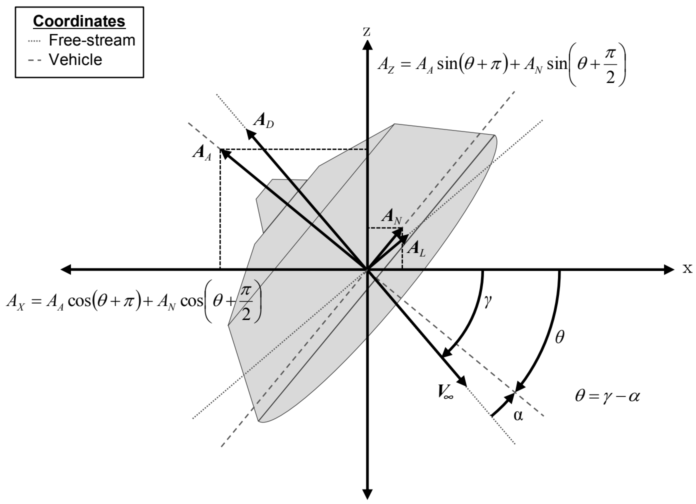

Figure 3. 3-DOF vehicle coordinate system shown in relation to the free-stream coordinate system and decomposed into the X-Z plane and also displaying the relationship between flight-path angle, γ, angle of attack, α, and incidence angle, θ

and Mach number by

$$M_\infty = V_{infty} / \sqrt{\gamma_c \frac{P_\infty}{\rho_\infty}} \tag{6}$$

and free-stream dynamic pressure as

$$q_\infty = \frac{1}{2}\rho_\infty V_\infty^2 = \frac{m_v A_A}{C_A S} \tag{7}$$

To gain independence of atmospheric models, these calculation can also be performed iteratively to converge to estimates.

B. MEADS Pressure Database

The MEADS pressure database is correlated to the aerodynamic database because of their reliance on the same CFD formulations. However, the discretization of points for pressure calculations is fundamentally different from the integration of pressures across the entire forebody that is performed to obtain coefficients for the aerodynamic database. The seven discrete pressure points on the heatshield can be seen in Fig. 4. As mentioned, the Shuttle Entry Air Data System provided the motivation to include MEADS on MSL, and the pressure reconstruction technique for MEADS is largely based on the method described by Pruett et al.[15]

The pressure reconstruction method begins by creating an interpolation model of the MEADS database, including the following variables: α, β, M_∞, q_∞, P_1-P_7, P_∞. Therefore

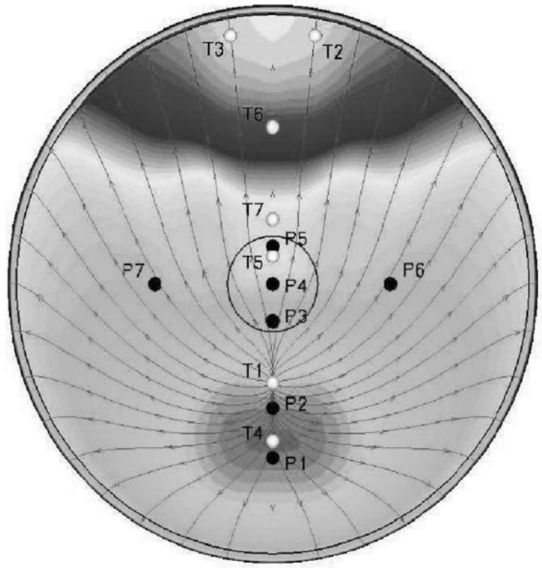

Figure 4. Locations of MEADS pressure transducers on the forebody of MSL heatshield are listed as P_1 through P_7.

the set of pressure measurements taken at each time step should correspond to a unique point within the model, and an optimization process is performed to create a time-series of estimated state variables. The specific calculations can be found in Karlgaard et al.[16]

C. Other Methods

There are other methods of trajectory reconstruction that have frequently been used with past missions but are beyond the scope of this paper. The extended Kalman filter (EKF) is a method that linearly filters all available data from pre-flight simulation and measurements obtained during flight in attempt to create the best estimated trajectory. The process can be found in Christian and Braun.[17] Another reconstruction technique that has been performed for the Other deterministic and statistical methods that have been developed through research and applied to past EDL reconstructions, and Desai presents an overview of such methods for Mars Pathfinder in a 2004 NASA technical report.[18]

IV. Methods of Reconciliation

In the context of post-flight trajectory reconstruction, reconciliation means being able to attribute deviations in trajectories to some lower-level physical meaning, i.e. determining causality for trajectory differences. This context of data reconciliation is closely related to the problem of calibration, where the objective is to determine values of parameters that will update a prediction function to account for actual experimental test data. As with calibration, a major difficulty is to ensure these calibration variables maintain their intended physical meaning, but the problem of trajectory reconciliation differs in that:

i) the calibration inputs for this problem will be used as diagnostic tools rather than improvements to the prediction function,
ii) the lessons learned will be used for a subsequent mission in which there will most likely be a slight deviation in vehicle shape, controls, physics, etc., and
iii) only one case of experimental data is available.

These inputs will be referred to as "reconciliation" inputs rather than calibration inputs to broaden the scope of the problem rather than limiting the possible solutions to methods of calibration. The vector, $\mathbf{w}$ will contain these inputs and will be more explicitly defined in the next section.

Techniques have been established in calibration and other fields that apply to this type of problem, but most assume the comparison of scalar or univariate time-series responses for stationary processes. Complications of trajectory reconciliation are highlighted by this assumption because a trajectory is a nonstationary process in which multivariate time-series data must be compared, and the ability for data reduction is limited. Because reconstruction requirements are imposed on the entire time-series, resolution is lost with data reduction techniques that transform responses to time-independent data. Trajectory reconciliation is also classified as an underdetermined problem when $p > 1$. These complications express the difficulty in reconciling differences between multivariate time-series and this section discusses the advantages and disadvantages of a variety of applicable methods. It is important to note that while these methods can be used as a general enabler for reconciliation problems, knowledge of the application is crucial for their effective utilization. In essence, results independent of knowledgable interpretation are less useful for the intended purpose of validation and improvement of simulation capabilities.

A. Optimization

Trajectory reconciliation is naturally posed as an optimization problem, where the minimization of a defined objective function or metric based on lower level inputs drives two different trajectories to match. This vector of reconciliation inputs, $\mathbf{w}$, is composed of uncertain variables described in Sections II and III. There are numerous metrics that can be used to quantify how well two trajectories compare to each other, and they are built upon the difference between state variables either at some significant point in the trajectory, $\mathbf{X}_{nom}(t = \tau) - \mathbf{X}'(t = \tau)$, or on the aggregate, $\mathbf{X}_{nom}(t) - \mathbf{X}'(t)$. In the former case for example, the minimization of distance between nominal and reconstructed landing sites would seem an obvious starting point objective function definition; however, this target-hitting optimization problem is non-unique and could converge to an infinite number of solutions within the uncertainty bounds of $\mathbf{w}$. For the latter case, the definition of $\mathbf{X}$ is crucial, because some formulations may artificially bias the metric value due to correlation of included state variables. For example, if the minimization problem is posed as

$$\underset{\mathbf{w}\in\mathbb{R}^p}{\operatorname{argmin}} f(\mathbf{w}) = \|\mathbf{X}'(\mathbf{w},t) - \mathbf{X}_{nom}(\mathbf{w},t)\| \tag{8}$$

where both state vectors are defined as a truncated version of Eqn. 1, or

$$\mathbf{X}_{nom} \equiv \mathbf{X}' \equiv (r, \phi_r, \theta_r, \alpha, \beta, \sigma, V_{xI}, V_{yI}, V_{zI})^T \tag{9}$$

then the minimization function is artificially biased due to the correlation between position and velocity. In an extreme case, the angle of incidence, see Fig. 3 could reduce the state vector to a single variable, which in 3 degrees of freedom is simply

$$\theta = \gamma - \alpha \tag{10}$$

where the flight-path angle, γ, accounts for altitude and downrange distance as well as their derivatives, and angle of attack, α, accounts for the angular velocity of the vehicle. These variables are very loosely correlated with atmospheric conditions, so it would therefore be beneficial to include dynamic pressure, q_∞, to more directly account for free-stream density, ρ_∞ and atmospheric pressure P_∞.

Since one of the main objectives for reconstruction efforts is estimation of state variables that coincide with the aerodynamics of the vehicle, the initial state vector for the optimization method was defined as $\mathbf{X} = (\alpha, \beta, \gamma, q_\infty)^T$. The aggregate minimization function in Eqn. 8 was tested using this state vector formulation and a constrained gradient-based minimization technique with undesirable conclusions. Optimally, the objective function would contain uniform convexity in p-dimensional space; however, Fig. 5 shows no such trend. This plot was generated by testing the metric on a pre-flight simulation function at the nominal case where $\mathbf{w} = [0]$. For visual purposes, only two dimensions of $\mathbf{w}$ were sampled, and the resulting surface of the objective metric shows no uniform increase as the components of $\mathbf{w}$ were further deviated from nominal conditions.

The application of the minimization technique offers some insight and shows the need for a significant amount of improvement before it can be considered a viable option. First, a gradient-based method may not be the most effective method of optimization, especially for problems with multiple local minima. Therefore, a more purely random technique could prove more useful, such as simulated annealing[19] or the genetic algorithm.[20] These techniques do not directly depend on a gradient function to guide the minimization. Secondly, the

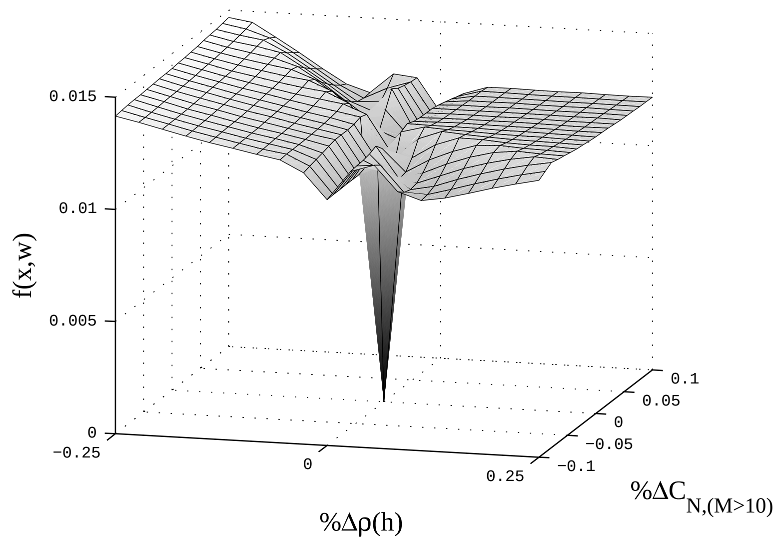

Figure 5. A two-dimensional sample space of the objective function in Eqn. 8 is shown against percentage change in the atmospheric density profile and percentage change of C_N above Mach 10. There is a large inverse spike at of the objective metric at the optimal solution; however, the general trend in the space is not decreasing toward that solution. Therefore, gradient-based techniques are inadequate for this objective function.

non-uniqueness of the objective function could be taken as a positive result in which the optimization method could be turned into a screening process. Particle swarm optimization is a technique in which the initial estimate of the input variables, $\mathbf{w}_0$, is generated randomly within the upper and lower bounds of $\mathbf{w}$ for a specified number of cases.[21] The final list of results for $\mathbf{w}$ could then be analyzed for plausibility by subject matter experts and filtered by other constraints in a systematic manner in order to mitigate subjectivity. Lastly, another option would be to tweak the objective function to include various combinations of point-performance and aggregate metrics in order to test for convexity. For example, different weighting scenarios could be placed on the aggregate formulation in Eqn. 8 for various Mach regimes. This essentially becomes a calibration of the model used during optimization, which could hinder performance at off-nominal or unexpected conditions. Although optimization might cognitively seem like a logical approach, much investigation of metric spaces is needed before optimization could be used as a viable option.

B. Calibration

Statistical calibration techniques for trajectory reconciliation are very attractive because distributions and confidence intervals can be calculated for the reconciliation variables, rather than purely deterministic values. One of these techniques that makes efficient use of prior information and expectation is Bayesian calibration. This method, based on the fundamentals of Bayes's approach to statistics, is generally motivated by the desire to improve simulation capabilities utilizing experimental data. The calibration itself blends the responses together, as they are modeled as distributions with mean and variance for both simulation and experimental data, where there is greater confidence in the distribution with smaller variance. Kennedy and O'Hagan classify the uncertainty that can exist in a simulation-test setup as:

Parameter Uncertainty upper and lower bounds of the inputs to the simulation and experiment,

Model Inadequacy "difference between the true mean value of the real world process and the code output at the true values of the inputs,"

Residual Variability variation in the response of the real-world process under identical input conditions,

Parametric Variability variation of output attributed to unspecified inputs,

Observation Error noise in observation of the actual process,

Code Uncertainty error attributed to the interpolation between actual sampled points in the p-dimensional input space.

and a calibration technique would optimally account for each of these sources of uncertainty.[22]

Bayesian calibration uses a procedure that estimates the distribution of each parameter contained within a calibration vector, $\mathbf{w}$. The ultimate goal in Kennedy and O'Hagan is to most accurately represent the real functional form of the problem, $\zeta(\mathbf{x})$, with the computational simulation form $\eta(\mathbf{x}, \mathbf{w})$ by variation of the vector $\mathbf{w}$, where $\mathbf{x}$ represents the normal inputs. The estimation of $\mathbf{w}$ and hyperparameters create an estimated distribution of the response, and Kennedy and O'Hagan develop a method for scalar responses.[22] Brown et al. further develop a Bayesian approach to calibration to handle responses that are time and spatially dependent.[23] In the application of rainfall estimation over time, the single site rainfall esimation is treated as a time-dependent linear model,

$$Y_t = A_t + B_t x_t + Z_t \qquad t = 1, \dots, T \tag{11}$$

where Y_t is the univariate time-series response, A_t and B_t are dynamic regression coefficients defined by stochastic processes which are in turn governed by Gaussian process state equations. These regression coefficients are determined by a Kalman filtering[24] algorithm which produces a likelihood function, and subsequently, the calibration parameters are determined as maximum likelihood estimators. A similar approach is presented by Higdon et al. for variations in space rather than time.[25]

Another calibration technique is presented by Horta et al. in the application of impact dynamic models for rotorcraft.[?] The problem is similar to EDL in that impact models are multivariate time-dependent and due to the overwhelming cost of testing, there is a limited amount of test allowable test cases. The calibration is set up as a three-step process of parameter selection and sensitivity by analysis of variance (ANOVA), study of uncertainty propagation, and optimization. The time-dependency issue is addressed by a surrogate modeling technique that represents the prediction function as a time-dependent linear model; however, the results that are obtained by the optimization strategy are purely deterministic values for the calibrated, or reconciled, variables.

Even though calibration methods address the issue of reconciliation of experimental data to simulation functions, this is an extreme case in that the number of experimental observations is limited to one case. Therefore, the goal is not to enhance the prediction function directly from observations, rather use that case to determine errors in assumptions or functional form of the simulation. To apply Bayesian calibration directly as a trajectory reconciliation technique, nonlinear dynamic modeling issues would need to be overcome, and research shows this issue has been addressed. Another issue would be quantifying a distribution to experimental responses for a single case. The imminent benefit of this approach, however, is the ability to determine reconciled variables in terms of distributions and probabilistic quantification and determination of confidence intervals.

C. Functional Data Analysis

Functional data analysis (FDA) can be used as method of trajectory reconciliation or an enabler for other methods. Observed data that is known to be a functional response of some input set is modeled by functional data analysis techniques, and various statistical properties of these data can also be explained using FDA. Ramsay and Silverman[26] present the ability to model functional data with functional linear models. These models take the form

$$y_i(t) = \alpha(t) + \int_{\tau_x} x_i(s)\beta(s,t)ds \tag{12}$$

where y_i is a functional observation of t, β is a regression function of t and s that expanded to functional form using basis functions, t is the functional dependent of the observation (typically time), s is the functional dependent of the covariate, x_i, and i designates a particular observation. This form of model could enable methods such as Bayesian calibration, but a more beneficial formulation would be if a functional linear model could directly relate the state variable of interest to the reconciliation variables, with a potential form

$$\mathbf{X}_i(t) = \alpha(t) + \int_{\tau_x} \mathbf{w}_i(s)\beta(s,t)ds \tag{13}$$

where $\mathbf{X}_i$ is a multivariate observation that is a function of time, t, and inherently the reconciliation variables, $\mathbf{w}$. Since the reconciliation variables are not necessarily functions, they could be driven to pseudo-functional form by defining s as the index of vector $\mathbf{w}$. This formulation allows for time-dependence statistical determination of distributions for reconciliation variables, or reconciled variables could be calculated deterministically by taking the inverse of the functional form in Eqn. 13. However, the methods described by Ramsay and Silverman assume a univariate response in the linear model, therefore further development is needed to handle multivariate state variable response, $\mathbf{X}_i$. An alternative to the linear model is the multi-layer perceptron for functional data presented in Rossi and Conan-Guez,[27] but the same drawback of a univariate response exists.

A helpful diagnostic approach in FDA is principal components analysis (PCA) for functional data. This methods decomposes data into orthogonal components that when coupled with variance-covariance structures can provide a significant amount of insight to correlation within the multivariate observations, which allows for easier interpretation of models. This could also replace or complement ANOVA methods that determine factor contribution to uncertainty or variance in a particular output or metric. Ultimately, FDA techniques would prove very useful to the problem of trajectory reconciliation dependent upon the development of techniques to expand the response beyond scalar values and univariate functions.

D. Pattern Recognition and Profile Matching

Statistical pattern recognition in this application is a significantly different approach from the previously described methods, and can be applied as a general classification or statistical quantification technique. Conceptually, pattern recognition for trajectory reconciliation is a problem of data mining. This method would entail the simulation and reconstruction models being sampled by a design of experiments (DOE), which would generate profiles of the state variables in time. This multivariate profile would be classified according to some learning algorithm, and the data obtained by DOE would build a classification model based on the profiles for each case. After reconstruction, multiple reconstructed trajectory profiles could be input to the classification model, and based on their respective features, would be classified by deviations in the vector $\mathbf{w}$. This method as proposed is not quantifiable but provides information to help subject matter experts in their engineering evaluations and benefit can be found in the classification guidelines.

A more quantifiable approach would be to complement pattern recognition with profile matching techniques. Vosselman and de Knecht present a method of profile matching with the use of Kalman filtering for automated map-building using a Kalman filter for road tracing.[28] This method could be adapted to use the state vector of interest and compare the estimation (nominal trajectory) with the actual case (reconstructed trajectory) or vice versa. These methods are conceptually feasible, but have not been adequately developed to make assessments on advantages and disadvantages of their application.

E. Recommendations

Assessing this review of reconciliation methods, it is suggested to combine a calibration approach using enabling functional data analysis techniques. The benefit of this approach would be the ability to specify distributions of reconciled variables, therefore introducing a factor of confidence and decreasing the risk of enhancing prediction capabilities based on possibly incorrect deterministic values of reconciled variables. It also provides possibilities to achieve greater insight to simulation and reconstruction models through functional data analysis techniques such as PCA.

In this anticipated method, either linear or MLP functional models will be developed for simulation and reconstruction based on their respective dominant sources of uncertainty, i.e. the components of $\mathbf{w}$ with the greatest contribution to variation in the state vectors $\mathbf{X}_{nom}$ and $\mathbf{X}'$ determined by functional ANOVA or PCA methods. The simulation model will represent the $\zeta(\mathbf{x}, \mathbf{w})$, and the reconstruction model will represent the a variation of the real process, $\eta^*(\mathbf{x}, \mathbf{w})$, that will be used to obtain variance measures for the data recorded during flight since there will only be one case of experimental observations under the vehicle and atmospheric conditions during EDL. A modified procedure based on the approach by Kennedy and O'Hagan will perform estimation of the posterior distributions of $\mathbf{X}$ and $\mathbf{w}$, where the enabling model will be a semi-parametric functional linear or MLP model of one response. Although this is not optimal, an appropriate response can be determined by examining correlation between state variables. More importantly, the entire time-series is represented with this formulation and can therefore support validation of the requirements imposed on trajectory reconstruction.

This suggested approach is anticipated to be quickly adapted to the trajectory reconciliation problem. Since Bayesian calibration methods have been developed for a number of case studies and functional MLP models have been demonstrated for time-dependent data, minimal research would be required for implementation. However, the functional data enabled Bayesian calibration method is an interim solution, because the bigger picture problem is developing the ability to regress multivariate time-dependent data.

A baseline process for performing trajectory reconciliation is presented in the next section. The demonstration uses mainly lower order approximations for techniques, but the process is defined that any combination of the methods just described can be incorporated.

V. Process Demonstration for 3-DOF Trajectory Model

A baseline process to perform reconciliation of differences between reconstructed trajectories is presented in this section. This process is demonstrated on a simplified 3-degree-of-freedom simulation to generate a nominal trajectory and investigate behavior of the state variables of interest at off-nominal conditions. This prediction model was also used to simulate measurements taken during actual flight, or the true trajectory. These measurements were analyzed by various reconstruction techniques, and the results from the baseline process of reconciliation, which can be seen in Fig. 6 are shown and discussed.

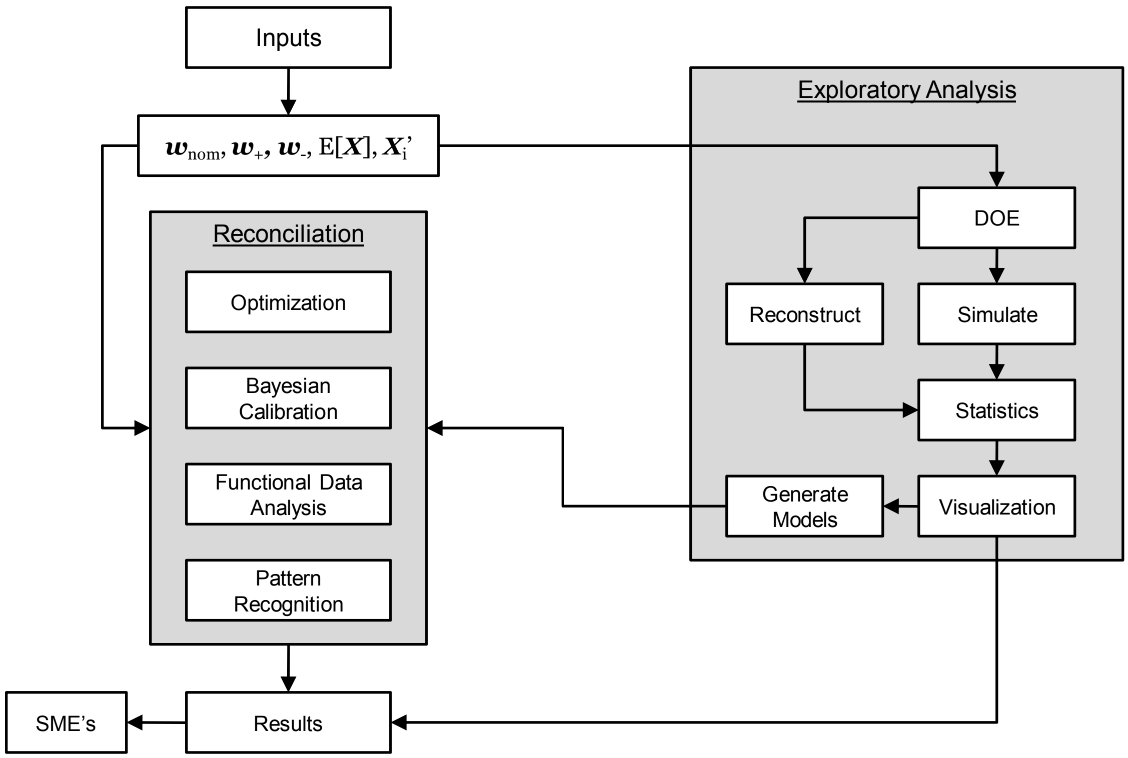

Figure 6. The baseline process for reconciling differences in EDL reconstructed trajectories is presented, where an exploratory analysis is performed for trajectory simulation and reconstruction and sent to the numerical methods mentioned in Section IV in order to obtain a vector of reconciled variables along with a multitude of visualization techniques.

A. Trajectory Simulation and Reconstruction

Trajectory reconciliation begins with the ability to investigate a particular simulation, and the model developed for this problem is of much lower fidelity than POST, containing a smaller number of inputs and more simplifying assumptions. However, the motivation for such a capability is for ease of interpretation for trends and sensitivities in uncertainty propagation and reconciliation. The trends witnessed in this study are representative capabilities of the reconciliation process itself and independent of the simulation. Therefore, it is anticipated that the process will generalize to accommodate varying levels of fidelity in modeling and apply to a number of interplanetary exploration missions rather than be limited to Mars.

Analysis begins by defining nominal conditions of the normal inputs, $\mathbf{x}$, and reconciliation inputs, $\mathbf{w}$, where

$$\mathbf{x} = \big(m_v, d_v, h_0, V_0, \gamma_0, \alpha_0, \rho(h), C_p/C_v, \varphi_{X,IMU}, \varphi_{Y/Z,IMU}, C_{N,(M_\infty<1.2)}, C_{N,(1.2\leq M<5)}\ , \dots$$
$$C_{N,(5\leq M<10)}, C_{N,(M\geq 10)}, C_{A,(M<1.2)}, C_{A,(1.2\leq M<5)}, C_{A,(5\leq M<10)}, C_{A,(M\geq 10)}\big)^T$$
$$\mathbf{x}_{nom} = (3200, 4.5, 100, 6500, 14.0, 6.0, 1.0\rho\,(h)\,, 1.4, 0, 0, f\,(M_\infty, \alpha)\,, \dots, f\,(M_\infty, \alpha))^T \tag{14}$$

and $\mathbf{w} = \%\Delta\mathbf{x}$ and $\mathbf{w}_{nom} = (0, \dots, 0)^T$. The allowable degrees of freedom in this simulation are translation in the X-Z plane and rotation about the Y-axis, and the equations of motion are a forward integration in time from the entry state designated at $h = 100$km to surface landing at $h = 0$. A flat Earth model is used in this formulation, with constant acceleration between time steps governing the equations of motion for a point mass:

$$x_{i+1} = x_i + V_i\Delta t + 0.5A_i\,(\Delta t)^2 \tag{15a}$$
$$V_{i+1} = V_i + A_i\Delta t \tag{15b}$$

These equations are decomposed in the X and Z axes, and A_i is the acceleration due to gravity,

$$g = g_0\left(\frac{r_p}{r_p + h}\right)^2 \tag{16}$$

as well as aerodynamic forces calculated using dynamic pressure and the aerodynamic database

$$q_\infty = \frac{1}{2}\rho V^2 \tag{17a}$$
$$A_N = q_\infty S C_N \tag{17b}$$
$$A_A = q_\infty S C_A. \tag{17c}$$

The values of C_N and C_A are determined by interpolation of the aerodynamic database in M_∞, which is calculated using an exponential atmospheric model

$$M_\infty = \frac{V_\infty}{\sqrt{\gamma\frac{P_{atm}}{\rho_{atm}}}} \tag{18}$$

where

$$P_\infty = P_0 \exp\left(-\frac{h}{H}\right) \tag{19a}$$
$$\rho_\infty = \rho_0 \exp\left(-\frac{h}{H}\right) \tag{19b}$$

and α, which is determined by the rotational equations of motion

$$\alpha_{i+1} = \alpha_i + \dot{\alpha}_i \Delta t + 0.5\ddot{\alpha}_i \left(\Delta t\right)^2 \tag{20a}$$

$$\dot{\alpha}_{i+1} = \dot{\alpha}_i + \ddot{\alpha}_i \Delta t \tag{20b}$$

$$\ddot{\alpha}_i = q_\infty C_m d_v S / I_{yy} \tag{20c}$$

where C_m is the pitching moment coefficient and also determined by interpolation of the aerodynamic database in M_∞ and α. This simulation is analyzed at nominal conditions to generate a nominal trajectory, and Fig. 7 shows a nominal Earth EDL trajectory for an entry vehicle with similar properties to MSL.

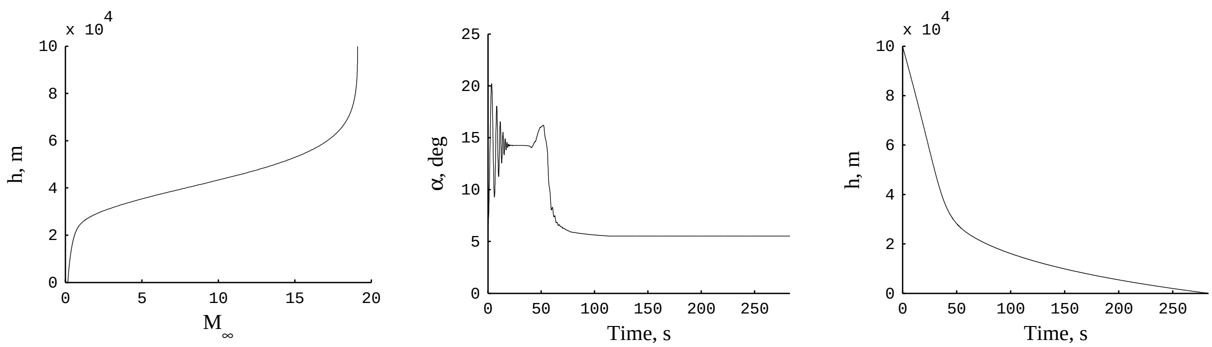

(a) M_∞ vs. Altitude (b) α vs. Time (c) Altitude vs. Time

Figure 7. Attributes of the nominal trajectory in this study are shown.

During the simulation, an algorithm records IMU accelerations and rates as well as pressure measurements from transducers 1-5 in Fig. 4 on the vehicle forebody vertical axis. In this manner, flight data can be simulated at nominal and off-nominal conditions through variation of $\mathbf{x}$ and $\mathbf{w}$. The simulated measurements are then processed by two reconstruction algorithms using the aerodynamic and pressure databases, respectively. To simplify, each method is blended with a simulation-based reconstruction method, where IMU measurements are integrated using the equations of motion to obtain velocity and altitude at each time step. Therefore, Mach number, M_∞, and dynamic pressure, q_∞, can be estimated with Eqns. 18 and 17a, respectively. Subsequently, α can be determined using the aerodynamic database by a reverse interpolation of the functional form, $\alpha = f\left(M_\infty, A_N/A_A\right)$.

In this case, pressure reconstruction is performed in a very similar manner as what is presented for the aerodynamic database. One major difference is that the input vector of reconciliation variables, $\mathbf{w}$, uses uncertainty coefficients for the pressure CFD model and is extended to include bias uncertainties attributed to hardware for the pressure measurements. Including these variables, the vector $\mathbf{w}$ becomes

$$\mathbf{w} = \%\Delta\left(m_v, \ldots, C_{P,(M<1.2)}, C_{P,(1.2\leq M<5)}, C_{P,(5\leq M<10)}, C_{P,(M\geq 10)}, P_1, P_2, P_3, P_4, P_5\right)^T. \tag{21}$$

where the C_P coefficients represent uncertainty in the CFD solutions that build the pressure database and $P_1 - P_5$ represent overall uncertainty in the transducer hardware which includes improper installation, surface contamination, inaccurate calibration, etc. This approach is simplified to deviate CFD pressures uniformly across the entire heatshield surface.

One of the driving factors that makes pressure reconstruction significantly different from the method presented in Section B is the difficulty in interpolation of the absolute pressure model. Figure 8(a) displays a representative interpolative absolute pressure model for port 1 against M_∞ and α, and it can be seen that the slope of P_1 versus α is relatively minuscule, especially at low Mach numbers which makes estimation of α extremely difficult. Therefore, the ratios P_5/P_3, P_5/P_2, and P_5/P_1, are calculated at each sampled point in the pressure database, and the interpolative model for P_5/P_3 is shown in Fig. 8(b). The other pressure ratio models are near identical, and there is much greater resolution in these models to estimate α, and they are more robust to deviations in M_∞. The method used in this example takes the mean value of the three α estimates.

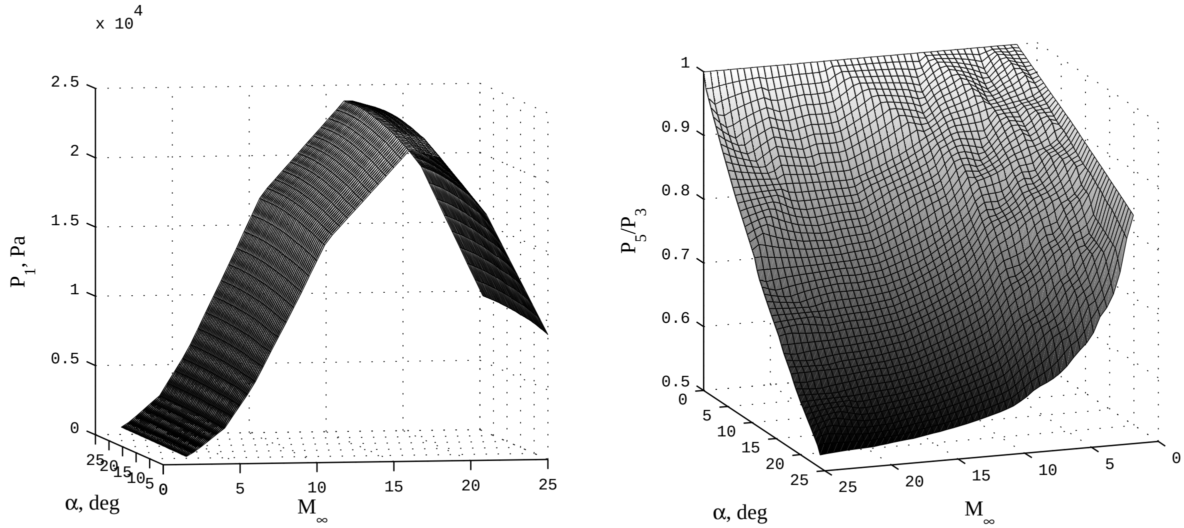

(a) P_1

(b) P_5/P_3

Figure 8. In this study, resolution for estimating alpha is greatly increased when using pressure ratios rather than absolute pressures during the reconstruction process. Estimation is also less sensitive to slight variations in Mach number.

Although the two methods presented are not identical to those in Section III, they are sufficient first order methods that provide two trajectories for comparison that are reconstructed from two different methods. The focus of this work is not to develop reconstruction methods themselves, rather gain insight to how those methods are different and how they can be improved and/or leveraged to validate pre-flight simulation capabilities. The next subsection describes the process of exploratory data analysis that will provide information that feeds into the reconciliation methods.

B. Exploratory Analysis

Visual and statistical representations of data provide a significant source of information to aid subject matter experts in the engineering judgment, but can also directly enable methods of reconciliation. Therefore, an exploratory analysis was performed on both simulation and reconstruction models to gain a greater insight to the data by:

- determining correlation between state variables,
- identifying dominant sources of uncertainty and screening input factors for importance,
- understanding how lower level uncertainties propagate to reconstruction of state variables,
- creating visual devices to support reconciliation and assessment of reconciled trajectories, and
- build statistical models for rapid model investigation, assessment of functional form, and to enable reconciliation methods such as Bayesian calibration.

This portion of the reconciliation process is also made difficult due to time dependence, because data reduction is often required in order to provide a visual representation of the data.

The first portion of the exploratory analysis is to determine the level correlation between state variables in both simulated and reconstructed forms. A matrix plot of correlation can be seen in Fig. 9 that displays the correlation between combination of state variables, and the variance of variable against itself. Using such a plot for visual analysis can pinpoint locations within the trajectory, certain Mach regimes for example, of particular interest. Large deviations in correlation between variables from simulation to reconstruction could indicate that the relationship between variables, and therefore possibly the functional form, has changed.

Another aspect of interest in trajectory reconciliation is how lower level uncertainty propagates through the simulation and reconstruction algorithms. Figures 10 and 11 display a method of visualization for uncertainty propagation of reconstructed variables. This analysis is performed using a 129-case fractional factorial design of experiments (DOE) to obtain first order trends and factor insights. A nominal trajectory was created in order to generate a simulated time-history of pressure and acceleration measurements. These measurements were sent to their corresponding reconstruction algorithm, and varying levels of uncertainty in the vector $\mathbf{w}$ were investigated as governed by the DOE. Random noise was ignored in this study in order to study the main effects of biases within the simulation and reconstruction models. Subsets of $\mathbf{w}$ can also be investigated in design of experiments in order to obtain a visual reference to the contribution of particular uncertainties to the reconstructed variables at each time step. By eliminating time-dependency, however, a more quantitative approach

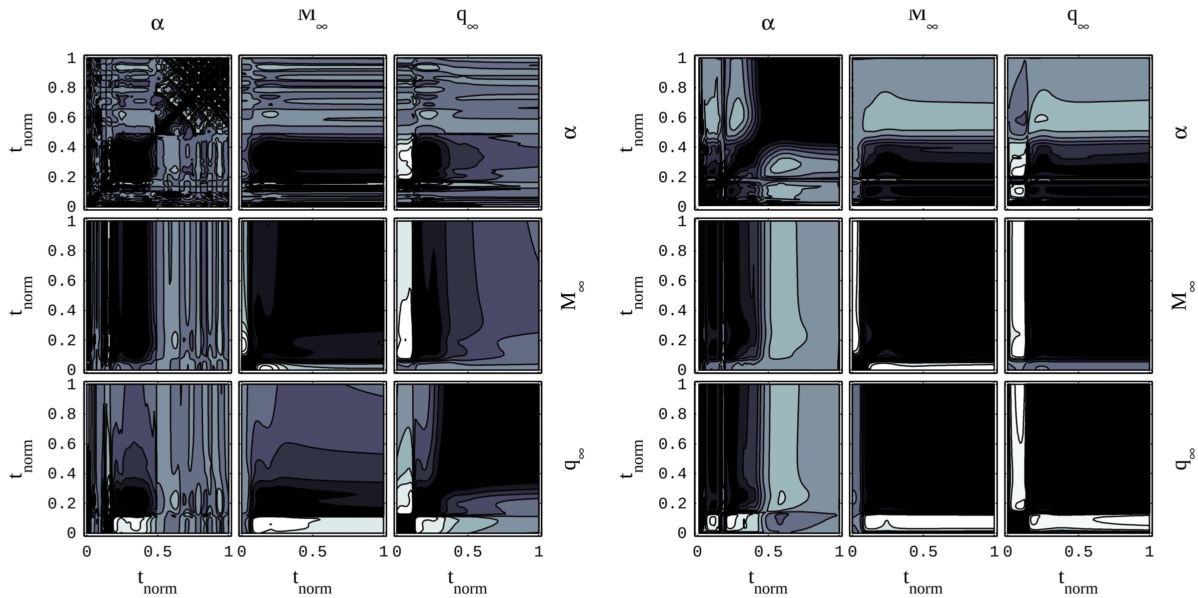

(a) Simulation

(b) Aerodynamic Reconstruction

Figure 9. Correlation of state variables is shown over the entire trajectory length (normalized in time). Black represents full correlation, i.e. Corr(X_1,X_2) = 1, whereas the white portions of the plots designate negative correlation, and gray areas have little to no correlation.

can be taken to determine the largest contributing factors to uncertainty propagation.

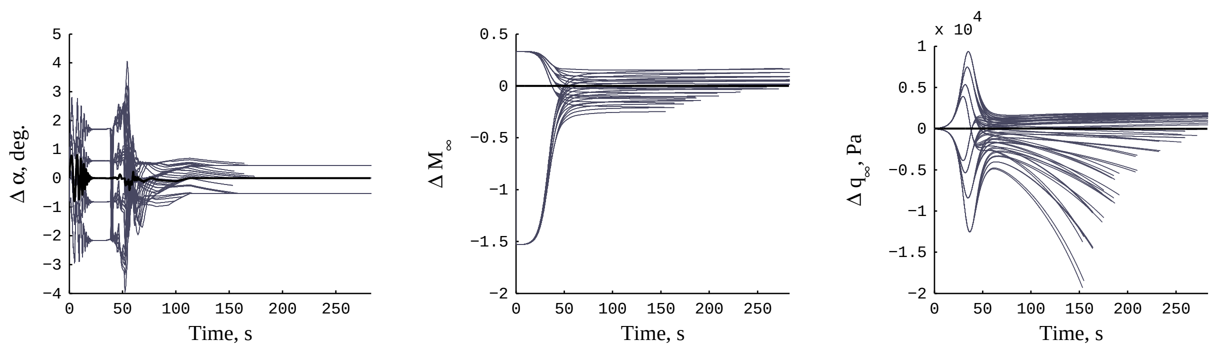

(a) Angle of Attack

(b) Mach

(c) Dynamic Pressure

Figure 10. A time-history of accelerations was produced during a simulation of nominal conditions, and the aerodynamic state variables were reconstructed using the aerodynamic database method. Uncertainty was introduced during this method, and the results above show the propagation of the uncertainty vector w.

Analysis of variance (ANOVA) quantitatively determines the contribution of factors to the variation of a response. Figure 12 shows ANOVA results for reconstructed variables from different methods of data reduction. The statistical mean, standard deviation, and absolute max values were determined for each case of the DOE and these aggregate values were analyzed using ANOVA. The results are relatively similar for each data reduction technique, and the dominant factors that contribute to uncertainty propagation are determined, but

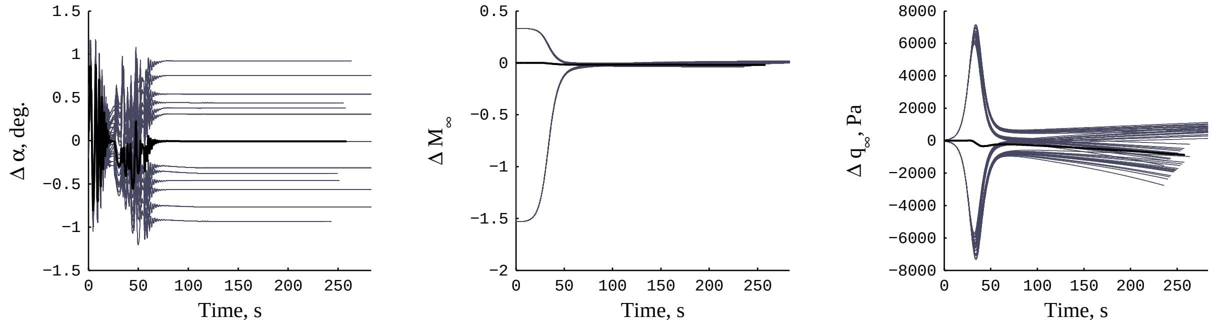

(a) Angle of Attack (b) Mach (c) Dynamic Pressure

Figure 11. Simulated pressure measurements were generated during a pre-flight simulation with nominal conditions, and uncertainty was introduced during the pressure database reconstruction process. The above plots display the propagation of that uncertainty to the reconstructed variables of interest.

it would be beneficial to quantify and visualize this information for multiple points along the trajectory. This analysis could be performed on segments of the trajectory through discretization, but there is also an option within the FDA techniques for functional analysis of variance (FANOVA). Other visual methods such as principal component analysis can be used for plotting data points against the two principal axes or generating a correlation circle plot can allow for easier interpretation of the data[a]; this and other helpful methods to gain insight to functional and time-series data can be found in Ramsay and Silverman[26] or from an exploratory data analysis perspective, see Hoaglin et al.[29]

C. Discussion

The quantitative reconciliation methods would be applied after interpretation of the visual methods and creation of surrogate models to enable quantitative analysis. The most beneficial and easy to implement approach is a Bayesian calibration method, and in order to maximize the potential of the approach and analyze the entire time-series of the trajectory, functional data models can be generated within the Bayesian process. Results from this type of analysis would be a mean value for the off-nominal estimated **w** along with the standard deviatoin or 3-σ confidence interval so that the risk in the analysis can also be assessed.

VI. Conclusions

Conclusions will be made in this section for the difficulties with reconciliation, the feasibility of a solution, assessment of exploratory methods, etc.

[a]These analyses and plots will be included in the next iteration of this report. Further interpretation of plots and general conclusions will also be made, while addressing modeling characteristics of the Bayesian approach in greater detail.

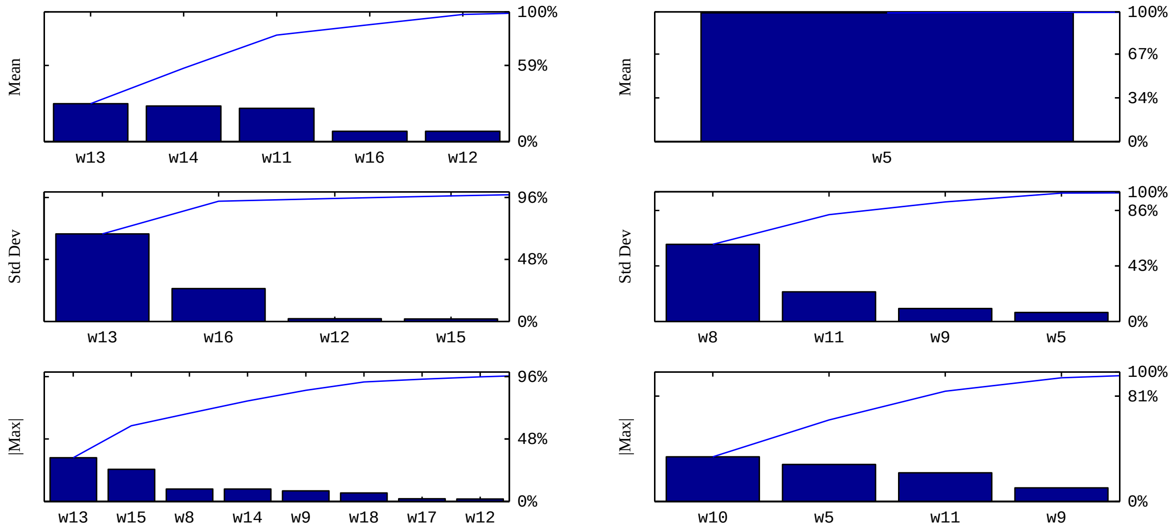

(a) Aerodynamic

(b) Pressure

Figure 12. Two Pareto charts are shown from the ANOVA analysis. The left side labels display the data reduction technique and the x-axis shows the index of w for each dominant factor.

Acknowledgments

The author would like to acknowledge Dr. Brian German, Dr. Peter Parker, and Mr. Sean Commo for their continued support and advisement throughout this entire project, as well as Mr. Mark Schoenenberger and Dr. Chris Kaarlgard for their helpful guidance in planetary entry, descent, and landing as well as providing supporting models for analysis.

References

[1]Braun, R. D. and Manning, R. M., "Mars exploration entry, descent and landing challenges," *Journal of Spacecraft and Rockets*, Vol. 44, No. 2, March-April 2007, pp. 310–323.

[2]Brauer, G., Cornick, D., and Stevenson, R., *Capabilities and applications of the program to optimize simulated trajectories (POST): program summary document*, Vol. 2770, National Aeronautics and Space Administration, 1977.

[3]Edquist, K. T., "Computations of Viking Lander Capsule Hypersonic Aerodynamics with Comparisons to Ground and Flight Data," *AIAA Atmospheric Flight Mechanics Conference and Exhibit*, 2006.

[4]Edquist, K. T., Desai, P. N., and Schoenenberger, M., "Aerodynamics for the mars Phoenix Entry Capsule," *AIAA/AAS Astrodynamics Specialist Conference and Exhibit*, 2008.

[5]Striepe, S., Way, D., Dwyer, A., and Balaram, J., "Mars Science Laboratory Simulations for Entry, Descent, and Landing," *Journal of Spacecraft and Rockets*, Vol. 43, 2006, pp. 311–323.

[6]Desai, P. N., Schoenenberger, M., and Cheatwood, F. M., "Mars Exploration Rover Six-Degree-of-Freedom Entry Trajectory Analysis," *Journal of Spacecraft and Rockets*, Vol. 43, No. 5, 2006, pp. 1019–1025.

[7]Braun, R. D., Powell, R. W., Engelund, W. C., and Gnoffo, P. A., "Mars Pathfinder Six-Degree-of-Freedom Entry Analysis," *Journal of Spacecraft and Rockets*, Vol. 32, 1995, pp. 993–1000.

[8]Euler, E., Adams, G., and Hopper, F., "Design and Reconstruction of the Viking Lander Descent Trajectories," *Journal of Guidance and Control*, Vol. 1, No. 5, 1978, pp. 372–378.

[9]Knocke, P., Wawrzyniak, G., Kennedy, B., Parker, T., Golombek, M., Duxbury, T., Kass, D., and Desai, P., "Mars Exploration Rovers landing dispersion analysis," *AIAA/AAS Astrodynamics Specialist Conference and Exhibit*, 2004.

[10]Desai, P. and Knocke, P., "Mars Exploration Rovers Entry, Descent, and Landing Trajectory Analysis," *Journal of the Astronautical Sciences*, Vol. 55, No. 3, 2007, pp. 311–324.

[11]Prince, J. L., Desai, P. N., Queen, E. M., and Grover, M. R., "Mars Phoenix Entry, Descent, and Landing Simulation Design and Modeling Analysis," *AIAA/AAS Astrodynamics Specialist Conference and Exhibit*, 2008.

[12]Prince, J. L., Desai, P. N., and Queen, E. M., "Entry, Descent, and Landing Operations Analysis for the Mars Phoenix Lander," *AIAA/AAS Astrodynamics Specialist Conference and Exhibit*, 2008.

[13]Queen, E. M., Prince, J. L., and Desai, P., "Multi-Body Modeling and Simulation for the Mars Phoenix Lander Entry, Descent and Landing," *AIAA/AAS Astrodynamics Specialist Conference and Exhibit*, 2008.

[14]Gnoffo, P. A., Braun, R. D., Weilmuenster, K. J., Mitcheltree, R. A., Engelund, W. C., and Powell, R. W., "Prediction and Validation of Mars Pathfinder Hypersonic Aerodynamic Database," *Journal of Spacecraft and Rockets*, Vol. 36, No. 3, May 1999, pp. 367–373.

[15]Pruett, C. D., Wolf, H., Heck, M. L., and Paul M. Siemers, I., "Innovative Air Data System for the Space Shuttle Orbiter," *Journal of Spacecraft and Rockets*, Vol. 20, 1983, pp. 61–69.

[16]Karlgaard, C. D., Beck, R. E., O'keefe, S. A., Paul M. Siemers, I., White, B. A., Engelund, W. C., and Munk, M. M., "Mars Entry Atmospheric Data System Modeling and Algorithm Development," *41st AIAA Thermophysics Conference*, 2009.

[17]Christian, J. A., Verges, A. M., and Braun, R. D., "Statistical Reconstruction of Mars Entry, Descent, and Landing Trajectories and Atmospheric Profiles," *AIAA Space 2007 Conference and Exposition*, 2007.

[18]Desai, P., Blanchard, R., and Powell, R., "Entry trajectory and atmosphere reconstruction methodologies for the Mars Exploration Rover mission," *International Workshop on Planetary Probe Atmospheric Entry and Descent Trajectory Analysis and Science*, Citeseer, 2004.

[19]Kirkpatrick, S., Gelatt, C., and Vecchi, M., "Optimization by simulated annealing," *Science*, Vol. 220, No. 4598, 1983, pp. 671.

[20]Goldberg, D., *Genetic algorithms in search, optimization and machine learning*, Addison-Wesley, 1989.

[21]Kennedy, J. and Eberhart, R., "Particle swarm optimization," *Neural Networks, 1995. Proceedings., IEEE International Conference on*, Vol. 4, IEEE, 1995, pp. 1942–1948.

[22]Kennedy, M. and O'Hagan, A., "Bayesian Calibration of Computer Models," *Journal of the Royal Statistical Society. Series B (Statistical Methodology)*, Vol. 63, No. 3, 2001, pp. 425–464.

[23]Brown, P., Diggle, P., Lord, M., and Young, P., "Space–time calibration of radar rainfall data," *Journal of the Royal Statistical Society: Series C (Applied Statistics)*, Vol. 50, No. 2, 2001, pp. 221–241.

[24]Kalman, R. et al., "A new approach to linear filtering and prediction problems," *Journal of basic Engineering*, Vol. 82, No. 1, 1960, pp. 35–45.

[25]Higdon, D., Kennedy, M., Cavendish, J., Cafeo, J., and Ryne, R., "Combining field data and computer

simulations for calibration and prediction," *SIAM Journal on Scientific Computing*, Vol. 26, No. 2, 2005, pp. 448–466.

[26]Ramsay, J. and Silverman, B., *Functional Data Analysis*, Springer-Verlag New York, 1997.

[27]Rossi, F. and Conan-Guez, B., "Functional multi-layer perceptron: a non-linear tool for functional data analysis," *Neural networks*, Vol. 18, No. 1, 2005, pp. 45–60.

[28]Vosselman, G. and de Knecht, J., "Road tracing by profile matching and Kalman filtering," *Automatic Extraction of Man-Made Objects from Aerial and Space Images*, Vol. 2, 1995.

[29]Hoaglin, D., Mosteller, F., and Tukey, J., *Understanding robust and exploratory data analysis*, Vol. 3, Wiley New York, 1983.